Steel and Composite Structures, *Vol. 35, No. 3 (2020) 405-413*
DOI: https://doi.org/10.12989/scs.2020.35.3.405

Buckling analysis of steel plates in composite structures with novel shape function

Ying Qin*, Ke-Rong Luo and Xin Yan

Key Laboratory of Concrete and Prestressed Concrete Structures of Ministry of Education, School of Civil Engineering, Southeast University, Nanjing, China

(*Received October 4, 2019, Revised April 14, 2020, Accepted April 24, 2020*)

Abstract. Current study on the buckling analysis of steel plate in composite structures normally focuses on applying finite element method to derive the buckling stress. However, it is time consuming, computationally complicated and tedious for general use in design by civil engineers. Therefore, in this study an analytical study is conducted to predict the buckling behavior of steel plates in composite structures. Hand calculation method was proposed based on energy principle. Novel buckling shapes with biquadratic functions along both loaded and unloaded direction were proposed to satisfy the boundary condition. Explicit solutions for predicting the critical local buckling stress of steel plate is obtained based on the Rayleigh-Ritz approach. The obtained results are compared with both experimental and numerical data. Good agreement has been achieved. Furthermore, the influences of key factors such as aspect ratio, width to thickness ratio, and elastic restraint stiffness on the local buckling performance are comprehensively discussed.

Keywords: local buckling; rotationally restrained; compression; steel plate; composite structure

1. Introduction

Steel-concrete composite structures have become increasingly applied in civil engineering applications. Composite structures offer excellent merits over conventional steel structures (Asgarian *et al.* 2012), especially in terms of high capacity, good ductility and satisfactory aesthetic appearance. Concrete-filled steel tubular (CFST) columns, as typical composite structures, are composed of infilled concrete and surrounding steel plate. The infilled concrete provides support to steel plate and prevents steel plate from buckling inward. However, it is vulnerable for steel plate to buckle outward due to the weak restraint along this direction under either compression or dynamic loading (Samani *et al.* 2014, Mirtaheri *et al.* 2017), which may eventually lead to progressive collapse in steel structures (Zoghi and Mirtaheri 2016, Mirtaheri *et al.* 2019).

The buckling analysis of pure plate (without rigid contact with concrete) has been studied by many researchers. Panahandeh-Shahraki *et al.* (2015) addressed thermoelastic buckling for laminated composite plates by Rayleigh-Ritz method. Bellifa *et al.* (2017) proposed a simple refined theory to analyze the buckling of functionally graded plates by using a new displacement function which includes undetermined integral variables. Dong *et al.* (2017) used one-dimensional mathematical method to address the local buckling analysis of an infinite thin rectangular laminated composite plate restrained by a tensionless Winkler foundation and subjected to uniform in-plane shear loading.

Belkacem *et al.* (2018) applied higher order shear deformation theory to study the hybrid laminated composite plates. Kolahdouzan *et al.* (2018) incorporated the refined Zigzag theory to model the buckling of sandwich micro plate. Xu *et al.* (2019) investigated the buckling behavior of sandwich plates by reporting their critical mechanical loads and the corresponding mode shapes.

The research on buckling analysis of steel plates in composite structures has been conducted by several researchers. Cai and Long (2009) and Long *et al.* (2016) derived the formulas for critical buckling stress of steel plate in concrete-filled tube column subjected to either axial or eccentric compressive loading. Li *et al.* (2016) conducted FE simulation to study the local buckling of bolted steel plate with different stiffener configurations. Kim *et al.* (2018) numerically investigated the bend-buckling strength of the web in longitudinally stiffened plate girder. Qin *et al.* (2017, 2018a, b) studied the buckling behavior of steel plate in composite structures under compression or combined compression and bending. Kanishchev and Kvocak (2019) presented theoretical, experimental and numerical study on buckling of concrete-filled tubular column under axial compression.

Numerical methods offer explicit solutions, but they are time consuming, computationally complicated and tedious for general use in design by civil engineers.

Similar to the steel plate in buckling-restrained braces (Gheidi *et al.* 2011, Mirtaheri *et al.* 2011, 2018), the buckling of steel plate in composite structures are restrained by rigid materials (Soltani *et al.* 2019, Shahsavari *et al.* 2019, Javani *et al.* 2019). The buckling of steel plates in CFST columns is quite different from that of pure plate. On the one hand, the steel plates in CFST columns are restrained to buckle between adjacent plates when subjected to compression. On

*Corresponding author, Associate Professor
E-mail: qinying@seu.edu.cn

ISSN: 1229-9367 (Print), 1598-6233 (Online)

the other hand, due to the restraint from concrete, the steel plate can only buckle outward.

To simulate this boundary condition, the steel plates are considered to be restrained along four edges by either adjacent plates or shear studs, as illustrated in Fig. 1. Some researchers (Millar and Mora 2015, Jana 2016) considered the steel plates to be simply-supported the four edges, while others (Stollenwerk and Wagner 2015) argued that it was more reasonable to consider that the loaded edges could offer a fixed boundary and the unloaded edges was simply-supported. It should be mentioned that the edges of the steel plate are restrained from rotation by surrounded components. However, the stiffness of adjacent component field may not be enough to provide a fixed boundary. Therefore, it is of importance to consider the case that the steel plates are restrained elastically along the four edges (Cai and Long 2009, Long *et al.* 2016, Qin *et al.* 2017, 2018a, b).

It should be noted that classical solutions for pure steel plate can be found in the shell and plate books. However, the deformed shape of steel plate in composite structures would be different from that of pure plate, which leads to different buckling stress. Furthermore, the steel plate is assumed to be either simply-supported or clamped in classical solutions, which cannot reflect the actual case. The work in this paper aims to address these two problems. In this paper, an effort is made to obtain the hand calculation formulas of local buckling stress of steel plates in composite structures, which assembles the method used by Cai and Long (2009), Long *et al.* (2016), and Qin *et al.* (2017, 2018a, b). The four edges of steel plate are assumed to be elastically restrained while two opposite edges are under compression, as shown in Fig. 1. New form of buckling shape was proposed to reflect the possible deflection of steel plate in contact with concrete. Explicit solutions for critical local buckling stress and critical aspect ratio are derived. The analytical results are then verified against available experimental and numerical data in the literature. Meanwhile, the influence of key factors, such as aspect ratio, width to thickness ratio, and rotational restraint stiffness, on the local buckling performance of steel plates was evaluated. The research in this paper can be considered as an alternative to the work by Cai and Long (2009) and Qin *et al.* (2017) by using a different buckling shape function to study the buckling issue of steel plate under axial compression.

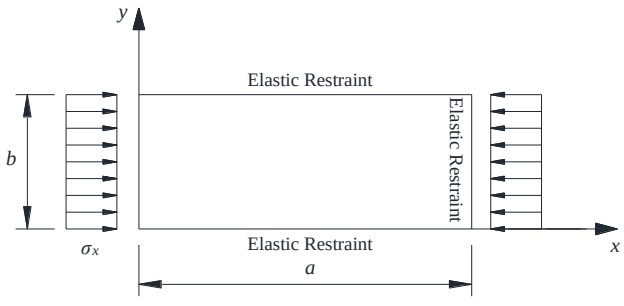

Fig. 1 Loading system and boundary condition of steel plate

2. Analytical derivation

2.1 Formulation for Elastically-Restrained Steel Plates

This section introduces the theoretical formulas for elastically-restrained steel plates. The related information can be found in many shell and plate books and the research by Cai and Long (2009), Long *et al.* (2016), and Qin *et al.* (2017, 2018a, b). A typical arrangement of steel plate elastically restrained is shown in Fig. 1. Normally, buckling occurs between adjacent supporting plates in concrete-filled tubular columns or between shear studs in composite walls. Therefore, the width of steel plate between two adjacent plates or two shear studs is denoted as b. The steel plate has the length of a and is subjected to in-plane compression. The resulted distributed stress along the x-direction is σ_x. According to the research by Timoshenko and Gere (1961), at the critical point when the plate starts to buckle under the load in the middle plane, the buckled shape should satisfy the requirement specified in Eq. (1). The flexural rigidity D can be calculated by Eq. (2).

$$\frac{\partial^4 w}{\partial x^4}+2\frac{\partial^4 w}{\partial x^2 \partial y^2}+\frac{\partial^4 w}{\partial y^4}=\frac{1}{D}\left(N_x\frac{\partial^2 w}{\partial x^2}+N_y\frac{\partial^2 w}{\partial y^2}+2N_{xy}\frac{\partial^2 w}{\partial x \partial y}\right) \quad (1)$$

$$D=\frac{Et^3}{12(1-\upsilon^2)} \quad (2)$$

The local buckling analysis of steel plate under uniaxial compression is conducted based on the Rayleigh-Ritz method. The total potential energy of the steel plate (Π) is required to be calculated on the basis of energy principle. It normally contains the strain energy and the work done by external force. For the analyzed steel plate with elastic restraint and under compression, the potential energy comprises the summation of the elastic potential energy due to the out-of-plane deflection (U_d), the potential energy of spring (U_s), and the work done by external applied compression (V), as illustrated in Eq. (3).

$$\Pi = U_d + U_s + V \quad (3)$$

Assuming the orthotropic behavior of steel plate, the elastic potential energy U_d during the plate deforming can be calculated by Eq. (4).

$$U_d = \frac{D}{2}\int_0^a\int_0^b\left\{\left(\frac{\partial^2 w}{\partial x^2}+\frac{\partial^2 w}{\partial y^2}\right)^2 - 2(1-\nu)\left[\frac{\partial^2 w}{\partial x^2}\frac{\partial^2 w}{\partial y^2} - \left(\frac{\partial^2 w}{\partial x \partial y}\right)^2\right]\right\}dxdy \quad (4)$$

As stated in section 1, The boundary condition of the steel plate is assumed to be elastic restraint against rotation along four edges. The restraint stiffness k_x and k_y at the loaded and unloaded edges, respectively, largely depends on the surrounded components. The energy U_s associated with the elastic springs is determined by Eq. (5).

$$U_s = \frac{1}{2}\int_0^a k_y \left(\frac{\partial w}{\partial y}\Big|_{y=0}\right)^2 dx + \frac{1}{2}\int_0^a k_y \left(\frac{\partial w}{\partial y}\Big|_{y=b}\right)^2 dx + \frac{1}{2}\int_0^b k_x \left(\frac{\partial w}{\partial x}\Big|_{x=0}\right)^2 dy + \frac{1}{2}\int_0^b k_x \left(\frac{\partial w}{\partial x}\Big|_{x=a}\right)^2 dy \quad (5)$$

It can be observed that the value of zero for k_x (or k_y) represents the case that the simply-supported boundary edges along the lines $y = 0$ and b (or $x = 0$ and a); while the value of infinity for k_x (or k_y) corresponds to the clamped boundary at $y = 0$ and b (or $x = 0$ and a). By choosing appropriate any other values for the elastic springs k_x and k_y, the boundary edges can be considered as elastic restraint against rotation.

The work V done by the compression N_x can be given by Eq. (6). N_x can be mathematically given by Eq. (7).

$$V = \frac{1}{2}\int_0^a \int_0^b N_x \left(\frac{\partial w}{\partial x}\right)^2 dxdy \quad (6)$$

$$N_x = -\sigma_x t \quad (7)$$

By substituting the appropriate buckling shape function into Eqs. (4)-(6), the total potential energy can be determined according to Eq. (3). In this way the buckling solution can be solved by Rayleigh-Rize method.

2.2 Buckling shape for the plate

It is important to choose a proper displacement function for the buckling shape when deriving the buckling strength of steel plate. From the literature review it can be observed that many of the proposed displacement functions by previous research are with too many variables to be determined, which will increase the complexity to solve the explicit solution. Furthermore, previous displacement functions cannot satisfy both loading and boundary conditions for steel plate in contact with concrete and subjected to compression.

In order to apply the Rayleigh-Ritz method to solve the buckling issue, the appropriate form of displacement function w should be proposed to well represent the out-of-plane buckled shape. For steel plate in touch with concrete, the only possibility of buckling shape is to buckle away from the concrete. Cai and Long (2009) and Long *et al.* (2016) proposed the shape function with a cosine function in the x direction and a biquadratic function in the y direction. Qin *et al.* (2017, 2018b) used the shape function with a combined sine and cosine function in the x direction and a biquadratic function in the y direction. Qin *et al.* (2018a) used the shape function with a combined sine and cosine function in both x and y directions.

Due to the uniaxial compression applied to the steel plate, the buckling shape should exhibit symmetry properties. Furthermore, for the sake of simplicity, the buckling shape function should include proper numbers of unknown coefficients in order to derive a closed-form solution. In this research, a new form of shape function was proposed. Biquadratic functions are uniquely combined as the buckled shape along both directions, as given by Eq. (8)

$$w(x,y) = C\left[\frac{y}{b} + \alpha_1\left(\frac{y}{b}\right)^2 + \alpha_2\left(\frac{y}{b}\right)^3 + \alpha_3\left(\frac{y}{b}\right)^4\right] \times \left[\frac{x}{a} + \beta_1\left(\frac{x}{a}\right)^2 + \beta_2\left(\frac{x}{a}\right)^3 + \beta_3\left(\frac{x}{a}\right)^4\right] \quad (8)$$

where C is a constant, and α_1, α_2, α_3, β_1, β_2 and β_3 are the constants to be determined which should satisfy both the boundary conditions and the requirement of compatibility.

As can be seen from Fig. 1, the steel plate with elastic restrained against rotation along four edges should satisfy the boundary condition as specified by Eq. (9).

$$w(0,y) = w(a,y) = 0 \quad (9a)$$

$$M_x(0,y) = -D\left(\frac{\partial^2 w}{\partial x^2}\right)_{x=0} = -k_x\left(\frac{\partial w}{\partial x}\right)_{x=0} \quad (9b)$$

$$M_x(a,y) = -D\left(\frac{\partial^2 w}{\partial x^2}\right)_{x=a} = +k_x\left(\frac{\partial w}{\partial x}\right)_{x=a} \quad (9c)$$

$$w(x,0) = w(x,b) = 0 \quad (10a)$$

$$M_y(x,0) = -D\left(\frac{\partial^2 w}{\partial y^2}\right)_{y=0} = -k_y\left(\frac{\partial w}{\partial y}\right)_{y=0} \quad (10b)$$

$$M_y(x,b) = -D\left(\frac{\partial^2 w}{\partial y^2}\right)_{y=b} = +k_y\left(\frac{\partial w}{\partial y}\right)_{y=b} \quad (10c)$$

It should be noted that the equations specified in Eqs. (9) and (10) will be used to obtain the values of unknown constants in Eq. (8). By taking the first-order and second-order partial derivative of w with respect to x and substituting them into Eq. (9), the unknown constants β_1, β_2, and β_3 can be determined as a function of the elastic spring (k_x) along the loaded edges as shown in Eq. (11).

$$\beta_1 = \frac{k_x a}{2D} \quad (11a)$$

$$\beta_2 = -\frac{2D + k_x a}{D} \quad (11b)$$

$$\beta_3 = \frac{2D + k_x a}{2D} \quad (11c)$$

Similarly, by taking the first-order and second-order partial derivative of w with respective to y and substituting them into either Eqs. (10), α_1, α_2, and α_3 can be expressed as a function of the elastic spring (k_y) along the unloaded edges as given in Eq. (12).

$$\alpha_1 = \frac{k_y b}{2D} \quad (12a)$$

$$\alpha_2 = -\frac{2D + k_y b}{D} \quad (12b)$$

$$\alpha_3 = \frac{2D + k_y b}{2D} \quad (12c)$$

By substituting Eq. (8) into Eqs. (4)-(6) and rearranging, the potential energy U, U_s, and V can be expressed in forms of the function with respect to the defined constants.

$$U = \frac{D}{2}\left[\frac{bC^2}{a^3}A_1B_1 + \frac{aC^2}{b^3}A_2B_2 + \frac{2\nu C^2}{ab}A_3B_3 + \frac{2(1-\nu)}{ab}A_4B_4\right] \tag{13a}$$

$$U_s = \frac{k_y aC^2[1+(1+2\alpha_1+3\alpha_2+4\alpha_3)^2]}{2b^2}B_2 + \frac{k_x bC^2[1+(1+2\beta_1+3\beta_2+4\beta_3)^2]}{2a^2}A_1 \tag{13b}$$

$$V = -\frac{C^2\sigma_x tbA_1B_4}{2a} \tag{13c}$$

where A_1, A_2, A_3, A_4, B_1, B_2, B_3 and B_4 are defined as

$$A_1 = \frac{1}{2}\alpha_1 + \frac{2}{5}\alpha_2 + \frac{1}{3}\alpha_3 + \frac{1}{5}\alpha_1^2 + \frac{1}{7}\alpha_2^2 + \frac{1}{9}\alpha_3^2 + \frac{1}{3}\alpha_1\alpha_2 + \frac{2}{7}\alpha_1\alpha_3 + \frac{1}{4}\alpha_2\alpha_3 + \frac{1}{3} \tag{14a}$$

$$A_2 = 4\alpha_1^2 + 12\alpha_2^2 + \frac{144}{5}\alpha_3^2 + 12\alpha_1\alpha_2 + 16\alpha_1\alpha_3 + 36\alpha_2\alpha_3 \tag{14b}$$

$$A_3 = \alpha_1 + 2\alpha_2 + 3\alpha_3 + \frac{2}{3}\alpha_1^2 + \frac{6}{5}\alpha_2^2 + \frac{12}{7}\alpha_3^2 + 2\alpha_1\alpha_2 + \frac{14}{5}\alpha_1\alpha_3 + 3\alpha_2\alpha_3 \tag{14c}$$

$$A_4 = 2\alpha_1 + 2\alpha_2 + 2\alpha_3 + \frac{4}{3}\alpha_1^2 + \frac{9}{5}\alpha_2^2 + \frac{16}{7}\alpha_3^2 + 3\alpha_1\alpha_2 + \frac{16}{5}\alpha_1\alpha_3 + 4\alpha_2\alpha_3 + 1 \tag{14d}$$

$$B_1 = 4\beta_1^2 + 12\beta_2^2 + \frac{144}{5}\beta_3^2 + 12\beta_1\beta_2 + 16\beta_1\beta_3 + 36\beta_2\beta_3 \tag{14e}$$

$$B_2 = \frac{1}{2}\beta_1 + \frac{2}{5}\beta_2 + \frac{1}{3}\beta_3 + \frac{1}{5}\beta_1^2 + \frac{1}{7}\beta_2^2 + \frac{1}{9}\beta_3^2 + \frac{1}{3}\beta_1\beta_2 + \frac{2}{7}\beta_1\beta_3 + \frac{1}{4}\beta_2\beta_3 + \frac{1}{3} \tag{14f}$$

$$B_3 = \beta_1 + 2\beta_2 + 3\beta_3 + \frac{2}{3}\beta_1^2 + \frac{6}{5}\beta_2^2 + \frac{12}{7}\beta_3^2 + 2\beta_1\beta_2 + \frac{14}{5}\beta_1\beta_3 + 3\beta_2\beta_3 \tag{14g}$$

$$B_4 = 2\beta_1 + 2\beta_2 + 2\beta_3 + \frac{4}{3}\beta_1^2 + \frac{9}{5}\beta_2^2 + \frac{16}{7}\beta_3^2 + 3\beta_1\beta_2 + \frac{16}{5}\beta_1\beta_3 + 4\beta_2\beta_3 + 1 \tag{14h}$$

Substituting Eqs. (13(a))-(13(c)) into Eq. (3), the total potential energy Π can be expressed by Eq. (15).

$$\Pi = \frac{D}{2}\left[\frac{bC^2}{a^3}A_1B_1 + \frac{aC^2}{b^3}A_2B_2 + \frac{2\nu C^2}{ab}A_3B_3 + \frac{2(1-\nu)}{ab}A_4B_4\right] - \frac{C^2\sigma_x tbA_1B_4}{2a} + \frac{k_y aC^2[1+(1+2\alpha_1+3\alpha_2+4\alpha_3)^2]}{2b^2}B_2 + \frac{k_x bC^2[1+(1+2\beta_1+3\beta_2+4\beta_3)^2]}{2a^2}A_1 \tag{15}$$

2.3 Explicit solution

Since the steel plate shall deform to a position that minimizes the total potential energy, the value of $\sigma_x t$ can be found by taking a first-order partial derivative of Eq. (15) with respect to C, as shown in Eq. (16).

$$\frac{\partial \Pi}{\partial C} = 0 \tag{16}$$

By substituting Eq. (15) into (16), the critical local buckling stress can be obtained by Eq. (17).

$$\sigma_x t = \frac{\pi^2 D}{b^2}\left[\frac{B_1}{\gamma^2\pi^2B_4} + \frac{\gamma^2A_2B_2}{\pi^2A_1B_4} + \frac{2\upsilon A_3B_3}{\pi^2A_1B_4} + \frac{2(1-\upsilon)A_4}{\pi^2A_1} + \frac{2\lambda_y\gamma^2[1+(1+2\alpha_1+3\alpha_2+4\alpha_3)^2]B_2}{\pi^2A_1B_4} + \frac{2\lambda_x[1+(1+2\beta_1+3\beta_2+4\beta_3)^2]}{\pi^2\gamma^2B_4}\right] = \frac{k\pi^2D}{b^2} \tag{17}$$

where γ =aspect ratio ($\gamma = a/b$); k =elastic local buckling coefficient and can be expressed by Eq. (18); λ_x and λ_y are the restraining factors along loaded and unloaded edges, respectively, as defined in Eqs. (19(a)) and (19(b)).

$$k = \frac{B_1}{\gamma^2\pi^2B_4} + \frac{\gamma^2A_2B_2}{\pi^2A_1B_4} + \frac{2\nu A_3B_3}{\pi^2A_1B_4} + \frac{2(1-\upsilon)A_4}{\pi^2A_1} + \frac{2\lambda_y\gamma^2[1+(1+2\alpha_1+3\alpha_2+4\alpha_4)^2]B_2}{\pi^2A_1B_4} + \frac{2\lambda_x[1+(1+2\beta_1+3\beta_2+4\beta_3)^2]}{\pi^2\gamma^2B_4} \tag{18}$$

$$\lambda_x = \frac{k_x a}{2D} \tag{19a}$$

$$\lambda_y = \frac{k_y b}{2D} \tag{19b}$$

As can be observed in Eq. (18), the elastic local buckling coefficient k is the function of aspect ratio γ. In order to get the critical local buckling coefficient k_{cr}, which should be the lower bound of Eq. (18), Eq. (18) is taken partial derivative with respect to γ and setting the result equal to zero. In this way the critical aspect ratio γ_{cr} is given by Eq. (20).

$$\gamma_{cr} = \left\{\frac{A_1B_1 + 2\lambda_x A_1[1 + (1 + 2\beta_1 + 3\beta_2 + 4\beta_3)^2]}{A_2B_2 + 2\lambda_y B_2[1 + (1 + 2\alpha_1 + 3\alpha_2 + 4\alpha_3)^2]}\right\}^{\frac{1}{4}} \quad (20)$$

Therefore, the critical local buckling coefficient k_{cr} can be obtained by substituting Eq. (20) into Eq. (17). The critical local buckling stress of the steel plate (σ_{cr}) under compressive load and with elastic restraint along four edges can be determined by substituting the function expression of k_{cr} and D into Eq. (17), which can be eventually expressed as Eq. (21).

$$\sigma_{cr} = \frac{k_{cr}\pi^2 E}{12(1-\nu^2)(b/t)^2} \quad (21)$$

3. Verification

In this section, the explicit solution for local buckling of steel plate in contact with concrete and under uniaxial compression, as given by Eq. (18), is simplified into several special cases. The obtained results from this research are compared with available analytical solutions and experimental data, which can indirectly verify the accuracy of the proposed method.

3.1 Case 1: CC Steel Plate

CC steel plate means the steel plate is clamped along both loaded and unloaded edges, which leads to $k_x \to \infty$ and $k_y \to \infty$. The value of critical aspect ratio $\gamma_{cr} = 1.0$ can then be obtained by Eq. (20). By substituting the value of γ_{cr} into Eq. (18), the value of critical local buckling coefficient $k_{cr} = 10.94$ can be obtained. This result is close to $k_{cr} = 9.81$ obtained by Liang *et al.* (2007) through the finite element buckling analysis, $k_{cr} = 9.99$ recommended by Bridge and O'Shea (1998) based on finite strip analysis, and $k_{cr} = 10.32$ suggested by Long *et al.* (2016). It can also be found that the proposed method slightly overestimates the buckling stress. Substituting the value of $k_{cr} = 10.94$ into Eq. (21) gives the critical local buckling stress as shown in Eq. (22).

$$\sigma_{cr} = \frac{10.94\pi^2 E}{12(1-\nu^2)(b/t)^2} \quad (22)$$

3.2 Case 2: CS Steel Plate

CS steel plate means the steel plate is clamped along the loaded edges while simply-supported along the unloaded edges, which leads to $k_x \to \infty$ and $k_y = 0$. The value of critical aspect ratio $\gamma_{cr} = 1.51$ can then be obtained by Eq. (20). By substituting the value of $\gamma_{cr} = 1.51$ into Eq. (18), the value of critical local buckling coefficient $k_{cr} = 5.74$ can be calculated. This result is close to $k_{cr} = 5.46$ proposed by Long *et al.* (2016). It should be noted that the method by Long *et al.* (2016) is closer to the exact solution, since both solutions by Long *et al.* (2016) and this research used the principle of minimum potential energy. Substituting the value of $k_{cr} = 5.74$ into Eq. (21) gives the critical local buckling stress as shown in Eq. (23).

$$\sigma_{cr} = \frac{5.74\pi^2 E}{12(1-\nu^2)(b/t)^2} \quad (23)$$

3.3 Case 3: SS Steel Plate

SS steel plate means the steel plate is simply-supported along both the loaded and the unloaded edges, which leads to $k_x = 0$ and $k_y = 0$. The value of critical aspect ratio is $\gamma_{cr} = 1.0$ based on Eq. (20), and the corresponding value of critical local buckling coefficient is $k_{cr} = 4.00$ based on Eq. (18). This result is close to $k_{cr} = 3.59$ proposed by Qin *et al.* (2018a). Substituting the value of $k_{cr} = 4.00$ into Eq. (21) gives the critical local buckling stress as shown in Eq. (24).

$$\sigma_{cr} = \frac{\pi^2 E}{3(1-\nu^2)(b/t)^2} \quad (24)$$

3.4 Case 4: CK Steel Plate

CK steel plate indicates the steel plate is clamped along the loaded edges while elastically restrained along the unloaded edges. Plates with clamped loaded edges indicated the elastic spring $k_x \to \infty$. In order to determine the critical aspect ratio given in Eq. (20), the reasonable value of λ_y should be proposed. It should be noted that λ_y can be transformed into k_y based on Eq. (19(b)). Bleich (1952) used Eq. (25) to predict the value of λ_y for steel plate.

$$\lambda_y = \left(\frac{t_w}{t_f}\right)^3 \frac{r}{\rho} \quad (25)$$

$$r = 1 - \beta_r \left(\frac{t_f b_w}{t_w b_f}\right)^2 \quad (26)$$

$$\rho = \frac{1}{\pi}\tanh\left(\frac{\pi b_w}{4b_f}\right)\left[1 + \frac{\pi b_w/2b_f}{\sinh(\pi b_w/2b_f)}\right] \quad (27)$$

Where b_f = width of the calculated steel plate; t_f =thickness of the calculated steel plate; b_w = width of the supporting steel plate; t_w =thickness of the supporting steel plate; r =reduction factor for steel plate in contact with concrete; $\beta_r = 0.5$ is the reduction factor used for considering the beneficial restraining effects offered by concrete.

Uy (1998, 2001) and Mo *et al.* (2004) conducted extensive tests to investigate the local buckling behavior of steel plates restrained by concrete. The readers could refer to the references listed above for the detailed test information. The key parameters and the comparison between tests and proposed theoretical methods are given in Table 1.

As can be noticed in Table 1, the assumption that the steel plate is clamped along both loaded and unloaded edges provides much higher local buckling strength than the experimental results, which is on the unconservative side. Furthermore, the assumption that the steel plate is clamped along the loaded edges while simply-supported along the

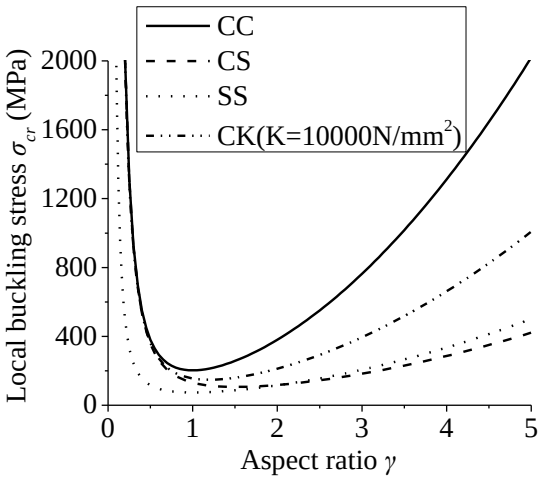

Fig. 2 Local buckling strength versus aspect ratio

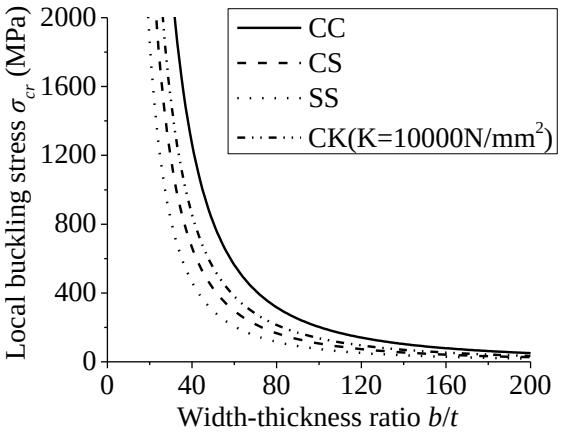

Fig. 3 Local buckling strength versus width to thickness ratio

unloaded edges offers relative low predictions and underestimates the actual buckling strength as expected. Meanwhile, the assumption that the steel plate is simply-supported along four edges provides the lowest values of local buckling stress.

It can also be found that it is more appropriate to assume that the steel plate is elastically restrained against rotation along the unloaded edges. The averaged ratio of predicted results based on equation in case 4 to experimental ones is 1.04 with the standard deviation of 0.10.

4. Discussion

4.1 Aspect ratio

The response between the aspect ratio and the local buckling strength is shown in Fig. 2. It can be seen that the CC steel plates are the most sensitive to the change in aspect ratio. For a steel plate with certain thickness, the local buckling strength σ_{cr} decreases shapely when the aspect ratio gradually grows. After reaching the critical value of γ, σ_{cr} smoothly goes up if the aspect ratio continues to grow. For CC, CS, SS, and CK steel plates, the minimum value of local buckling strength can be obtained when the aspect ratios γ equal 1.0, 1.5, 1.0, and 1.2, respectively. The corresponding buckling stresses are 203 MPa, 106 MPa, 74 MPa, and 148 MPa, respectively. This indicates that for steel plates with clamped boundary conditions along four edges or with simply-supported boundary conditions along four edges, square steel plate is more vulnerable to local buckling.

4.2 Width to thickness ratio

The relationship between width to thickness ratio and local buckling strength for steel plate with fixed aspect ratio is illustrated in Fig. 3. It can be found that the local buckling strength of steel plate is sensitive to the width to thickness ratio. The local buckling strength of steel plate steadily goes down with the increase in width to thickness ratio.

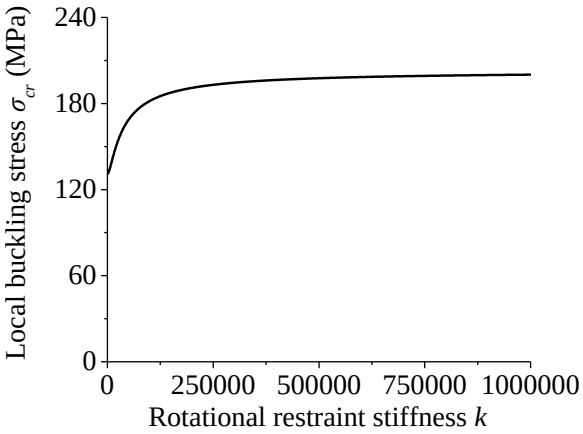

Fig. 4 Local buckling strength versus rotational restraint stiffness

For practical design in China, the yield strength of steel used in civil engineering is normally less than 400 MPa. If the steel plate is expected to yield before local buckling occurs, which means strength failure rather than stability failure dominates, the width to thickness ratio of the steel plate should be limited to $b/t \leq 45$ according to the plot in Fig. 3.

4.3 Rotational restraint stiffness

It can be observed from Fig. 4 that, the behavior of local buckling for steel plate is largely affected by the rotational restraint stiffness. Steel plate with extremely small rotational restraint stiffness represents the simply-supported boundary condition, while that with infinitely large rotational restraint stiffness denotes the clamped boundary condition. It demonstrates that the local buckling performance of steel plate under compression is more sensitive to the rotational restraint stiffness when the stiffness of adjacent component

Table 1 Comparison between test results and proposed equations

Specimen No.	b	t_f	t_w	$\sigma_{cr,e}$	Case 1 by Eq.(22)		Case 2 by Eq.(23)		Case 3 by Eq. (24)		Case 4		Reference
	mm	mm	mm	MPa	σ_{cr1}(MPa)	$\sigma_{cr1}/\sigma_{cr,e}$	σ_{cr2}(MPa)	$\sigma_{cr2}/\sigma_{cr,e}$	σ_{cr3}(MPa)	$\sigma_{cr3}/\sigma_{cr,e}$	$\sigma_{cr,t}$(MPa)	$\sigma_{cr,t}/\sigma_{cr,e}$	
LB7	240	3	3	200	317	1.59	166	0.83	116	0.58	195	0.99	Uy (1998)
LB9	300	3	3	120	203	1.69	106	0.88	74	0.62	125	1.06	
FB1	360	3	3	93.4	141	1.51	74	0.79	51	0.55	87	0.94	Uy (2001)
FB2	420	3	3	79.9	103	1.29	54	0.68	38	0.48	64	0.81	
FB3	480	3	3	43.7	79	1.81	42	0.96	29	0.66	49	1.12	
FB4	540	3	3	38.8	63	1.62	33	0.85	23	0.59	39	1.01	
SCC2	200	3	3	246	456	1.85	239	0.97	167	0.68	281	1.16	Mo *et al.* (2004)
SCC6	200	2	2	118	203	1.64	106	0.90	74	0.63	125	1.07	
Average						1.67		0.86		0.60		1.01	
Standard deviation						0.17		0.09		0.06		0.10	

Note: $\sigma_{cr,e}$ = local buckling strength according to the experimental recordings; σ_{cr1}, σ_{cr2}, σ_{cr3} =local buckling strength calculated by Eqs. (22)-(24), respectively; $\sigma_{cr,t}$ = local buckling strength based on case that the steel plate is clamped along the loaded edges while elastically-restrained along the unloaded edges

field is weak. Furthermore, if rotational restraint has been strong enough, the local buckling strength cannot be greatly raised by increasing rotational restraint stiffness. This observation is in consistant with that obtained by Qin *et al.* (2018b).

5. Conclusions

This research revisited a topic of plate buckling behavior, a classical yet critical issue, and presented analytical solutions based on an energy approach. Analytical procedures for estimating the local buckling strength of steel plate under compression has been developed in this research. The proposed method is based on Rayleigh-Rize method, which assembles the method used by Cai and Long (2009), Long *et al.* (2016), and Qin *et al.* (2017, 2018a, 2018b). Both the loaded and unloaded edges are assumed to be elastically restrained against rotation. The new buckling function combining biquadratic functions along both directions has been developed. Explicit solutions are obtained according to the energy principle. The obtained solution is simplified into several cases such as CC steel plate, CS steel plate, SS steel plate and CK steel plate. The results are compared to the available experimental data and previous solutions by either analytical or finite element method. Furthermore, the influences of several key parameters on the local buckling strength of steel plate has been comprehensively evaluated. The following conclusions may be drawn based on the research in this paper.

(1) The shape function with combined biquadratic functions is capable of representing the buckling characteristics of steel plate in composite structures. Both the requirement for boundary conditions and compatibility can be satisfied.

(2) The proposed hand calculation procedure is able to predict the local buckling performance of steel plate in composite structures. Good agreement has been found between the available experimental data, previous solutions and the predictions by the proposed method.

(3) The CC and SS steel plates with square shapes (aspect ratio equals zero) are more vulnerable to local buckling. The requirement for width to thickness ratio of the steel plate can be limited to $b/t \leq 45$ to avoid possible local buckling before yielding. Meanwhile, rotational restraint stiffness has significant influence on local buckling of steel plate when the stiffness of adjacent component field is weak.

It should be mentioned that the analytical solutions for the buckling of steel plates in composite structures are complicated. For steel plate with stiffeners, the research in this paper can be applied. In this case, the steel plate can be divided into several small steel plates. Each small steel plate can be considered as elastically restrained by the surrounded stiffeners. However, for steel plate with openings, the current research cannot be used to solve the problem. Finite element simulations are recommended to be used to obtained the buckling solutions.

Acknowledgments

This work is sponsored by the Natural Science Foundation of Jiangsu Province (Grant No. BK20170685), and the National Key Research and Development Program of China (Grant No. 2017YFC0703802). The authors also appreciate the financial support provided by Jiangsu Overseas Visiting Scholar Program for University Prominent Young & Middle-aged Teachers and Presidents.

References

Asgarian, B., Khazaee, H. and Mirtaheri, M. (2012), "Performance evaluation of different types of steel moment resisting frames subjected to strong ground motion through incremental dynamic analysis", *Int. J. Steel Struct.*, **12**(3), 363-379. https://doi.org/10.1007/s13296-012-3006-6.

Belkacem, A., Tahar, H.D., Abderrezak, R., Amine, B.M., Mohamed, Z. and Boussad, A. (2018), "Mechanical buckling analysis of hybrid laminated composite plates under different boundary conditions", *Struct. Eng. Mech.*, **66**(6), 761-769. https://doi.org/10.12989/sem.2018.66.6.761.

Bellifa, H., Bakora, A., Tounsi, A., Bousahla, A.A. and Mahmoud, S.R. (2017), "An efficient and simple four variable refined plate theory for buckling analysis of functionally graded plates", *Steel Compos. Struct.*, **25**(3), 257-270. https://doi.org/10.12989/scs.2017.25.3.257.

Bridge, R.Q. and O'Shea, M.D. (1998), "behaviour of thin-walled steel box sections with or without internal restraint", *J. Constr. Steel Res.*, **47**, 73-91. https://doi.org/10.1016/S0143-974X(98)80103-X.

Bleich, F. (1952). Buckling strength of metal structures, McGraw-Hill (New York).

Cai, J. and Long, Y.L. (2009), "Local buckling of steel plates in rectangular CFT columns with binding bars", *J. Constr. Steel Res.*, **65**, 965-972. https://doi.org/10.1016/j.jcsr.2008.07.025.

Dong, J.H., Ma, X., Zhuge, Y. and Mills, J.E. (2017), "Shear buckling analysis of laminated plates on tensionless elastic foundations", *Steel Compos. Struct.*, **24**(6), 697-709. https://doi.org/10.12989/scs.2017.24.6.697.

Gheidi, A., Mirtaheri, M., Zandi, A.P. and Alanjari, P. (2011), "Effect of filler material on local and global behaviour of buckling-restrained braces", *Struct. Des. Tall Spec.l Build.*, **20** (6), 700-710. https://doi.org/10.1002/tal.555.

Jana, P. (2016), "Optimal design of uniaxially compressed perforated rectangular plate for maximum buckling load", *Thin Wall. Struct.*, **103**, 225-230. https://doi.org/10.1016/j.tws.2015.12.027.

Javani, R., Bidgoli, M.R. and Kolahchi, R. (2019), "Buckling analysis of plates reinforced by Graphene platelet based on Halpin-Tsai and Reddy theories", *Steel Compos. Struct.*, **31**(4), 419-426. https://doi.org/10.12989/scs.2019.31.4.419.

Kanishchev, R. and Kvocak, V. (2019), "Local buckling of rectangular steel tubes filled with concrete", *Steel Compos. Struct.*, **31**(2), 201-216. https://doi.org/10.12989/scs.2019.31.2.201.

Kim, H.S., Park, Y.M., Kim, B.J. and Kim, K. (2018), "Numerical investigation of buckling strength of longitudinally stiffened web of plate girders subjected to bending", *Struct. Eng. Mech.*, **65**(2), 141-154. https://doi.org/10.12989/sem.2018.65.2.141.

Kolahdouzan, F., Arani, A.G. and Abodollahian, M. (2018), "Buckling and free vibration analysis of FG-CNTRC-micro sandwich plate", *Steel Compos. Struct.*, **26**(3), 273-287. https://doi.org/10.12989/scs.2018.26.3.273.

Liang, Q.Q., Uy, B. and Liew, J.Y.R. (2007), "Local buckling of steel plates in concrete-filled thin-walled steel tubular beam–columns", *J. Constr. Steel Res.*, **63**, 396-405. https://doi.org/10.1016/j.jcsr.2006.05.004.

Long, Y.L., Wan, J. and Cai, J. (2016), "Theoretical study on local buckling of rectangular CFT columns under eccentric compression", *J. Constr. Steel Res.*, **120**, 70-80. https://doi.org/10.1016/j.jcsr.2015.12.029.

Li, L.Z., Jiang, C.J., Jia, L.J.and Lu, Z.D. (2016), "Local buckling of bolted steel plates with different stiffener configuration", *Eng. Struct.*, **119**, 186-197. https://doi.org/10.1016/j.engstruct.2016.03.053.

Millar, F. and Mora, D. (2015), "A finite element method for the buckling problem of simply supported Kirchhoff plates", *J. Comput. Appl. Math.*, **286**, 68-78. https://doi.org/10.1016/j.cam.2015.02.018.

Mirtaheri, M., Gheidi, A., Zandi, A.P., Alanjari, P. and Samani, H.R. (2011), "Experimental optimization studies on steel core lengths in buckling restrained braces", *J. Constr. Steel Res.*, **67**(8), 1244-1253. https://doi.org/10.1016/j.jcsr.2011.03.004.

Mirtaheri, M., Amini, M. and Khorshidi, H. (2017),. "Incremental dynamic analyses of concrete buildings reinforced with shape memory alloy", *Steel Compos. Struct.*, **23**(1), 95-105. https://doi.org/10.12989/scs.2017.23.1.095.

Mirtaheri, M., Sehat, S. and Nazeryan, M. (2018), "Improving the behavior of buckling restrained braces through obtaining optimum steel core length", *Struct. Eng. Mech.*, **65**(4), 401-408. https://doi.org/10.12989/sem.2018.65.4.401.

Mirtaheri, M., Emami, F., Zoghi, M.A. and Salkhordeh, M. (2019). "Mitigation of progressive collapse in steel structures using a new passive connection", *Struct. Eng. Mech.*, **70**(4), 381-394. https://doi.org/10.12989/sem.2019.70.4.381.

Mo, S.X., Zhao, R.D. and Zhong, X.G. (2004), "Local buckling research on concrete filled square steel box member", *J. Hunan Uni. Sci. Tech.*, **19**, 43-46.

Panahandeh-Shahraki, D., Mirdamadi, H.R. and Vaseghi, O. (2015), "Thermoelastic buckling analysis of laminated piezoelectric composite plates", *Int. J. Mech. Mater. Des.*, **11**(4), 371-385. https://doi.org/10.1007/s10999-014-9284-8.

Qin, Y., Lu, J.Y. and Cao, S. (2017), "Theoretical study on local buckling of steel plate in concrete-filled tube column under axial compression", *ISIJ Int.*, **57**(9), 1645-1651. http://dx.doi.org/10.2355/isijinternational.ISIJINT-2016-755.

Qin, Y., Du, E.F., Li, Y.W. and Zhang, J.Z. (2018a), "Local buckling of steel plates in composite structures under combined bending and compression", *ISIS Int.*, **58**(11), 2133-2141. https://doi.org/10.2355/isijinternational.ISIJINT-2018-202

Qin, Y., Shu, G.P., Du, E.F. and Lu, R.H. (2018b), "Buckling analysis of elastically-restrained steel plates under eccentric compression", *Steel Compos. Struct.*, **29**(3), 379-389. https://doi.org/10.12989/scs.2018.29.3.379.

Samani, H.R., Mirtaheri, M., Zandi, A.P. and Bahai, H. (2014), "The effects of dynamic loading on hysteretic behavior of frictional dampers", *Shock Vib.*, **2014**, 181534. https://doi.org/10.1155/2014/181534.

Shahsavari, D., Karami, B. and Janghorban, M. (2019), "On buckling analysis of laminated composite plates using a nonlocal refined four-variable model", *Steel Compos. Struct.*, **32**(2), 173-187. https://doi.org/10.12989/scs.2019.32.2.173.

Soltani, K., Bessaim, A., Houari, M.S.A., Kaci, A., Benguediab, M., Tounsi, A. and Alhodaly, M.S. (2019), "A novel hyperbolic shear deformation theory for the mechanical buckling analysis of advanced composite plates resting on elastic foundations", *Steel Compos. Struct.*, **30**(1), 13-29. https://doi.org/10.12989/scs.2019.30.1.013.

Stollenwerk, K. and Wagner, A. (2015), "Optimality conditions for the buckling of a clamped plate", *J. Math. Anal. Appl.*, **432**(1), 254-273. https://doi.org/10.1016/j.jmaa.2015.06.035.

Timoshenko, S.P., and Gere, J.M. (1961). Theory of Elastic Stability, 2nd edition, Mcgraw-Hill (New York).

Uy, B. (1998), "Local and post-local buckling of concrete-filled steel welded box columns", *J. Constr. Steel Res.*, **47**, 47-72. https://doi.org/10.1016/S0143-974X(98)80102-8.

Uy, B. (2001), "Local and postlocal buckling of fabricated steel and composite cross sections." *J. Struct. Eng.*, **127**, 666-677. https://doi.org/10.1061/(ASCE)0733-9445(2001)127:6(666)

Xu, K., Yuan, Y. and Li, M. (2019), "Buckling behavior of functionally graded porous plates integrated with laminated composite faces sheets", *Steel Compos. Struct.*, **32**(5), 633-642. https://doi.org/10.12989/scs.2019.32.5.633.

Zoghi, M.A. and Mirtaheri, M. (2016), "Progressive collapse analysis of steel building considering effects of infill panels", *Struct. Eng. Mech.*, **59**(1), 59-82. https://doi.org/10.12989/sem.2016.59.1.059.

CC